This document is the Accepted Manuscript version of a Published Work that appeared in final form as L.C. Giannossa, D. Cesari, E. Merico, A. Dinoi, A. Mangone, M.R. Guascito, D. Contini, Inter-annual variability of source contributions to PM10, PM2.5, and oxidative potential in an urban background site in the central mediterranean, Journal of Environmental Management 319 (2022) 115752, doi: https://doi.org/10.1016/j.jenvman.2022.115752

Graphical abstract

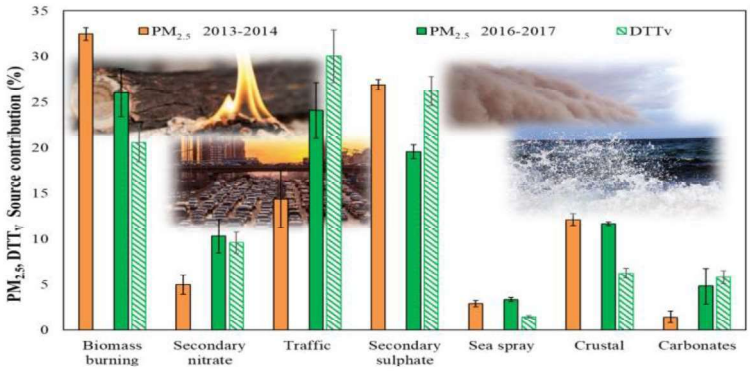

Highlights

- Source contributions have inter-annual variability higher for $PM_{2.5}$ than for PM_{10}.
- Inter-annual variability of crustal, carbonates, and sea spray were lower than 0.3% of PM.
- An increase of secondary nitrate and a decrease of sulphate in $PM_{2.5}$ was observed.
- DTT_V of $PM_{2.5}$ peaked in cold periods, instead DTT_V in $PM_{10\text{-}2.5}$ peaked in summer.
- DTT_V in $PM_{2.5}$ and in coarse ($PM_{10\text{-}2.5}$) fractions were influenced by different sources.

Inter-annual variability of source contributions to PM_{10}, $PM_{2.5}$, and oxidative potential in an urban background site in the central Mediterranean

Lorena Carla Giannossa[1], Daniela Cesari[2,*], Eva Merico[2], Adelaide Dinoi[2], Annarosa Mangone[1], Maria Rachele Guascito[2,3], Daniele Contini[2]

[1] University of Bari Aldo Moro, Department of Chemistry, I-70125 Bari,
[2]Italy National Research Council of Italy, Institute of Atmospheric Sciences and Climate (CNR-ISAC), Lecce, 73100, Italy
[3] Department of Environmental and Biological Sciences and Technologies (DISTEBA), University of Salento, Lecce, 73100, Italy.

* Corresponding author: d.cesari@isac.cnr.it

Abstract

Airborne particulate matter (PM) is studied because of its effects on human health and climate change. PM long-term characterisation allows identifying trends and evaluating the outcomes of environmental protection policies. This work is aimed to study the inter-annual variability of $PM_{2.5}$ and PM_{10} concentrations and chemical composition in an urban background site (Italy). A dataset of daily $PM_{2.5}$ and PM_{10} was collected in the period 2016-2017, including the content of OC, EC, major water-soluble ions, main metals, and compared to a similar dataset collected in the period 2013-2014. Oxidative potential using DTT assay (dithiothreitol) was evaluated and expressed in DTT_V as 0.39 nmol/min·m^3 in PM_{10} and 0.29 in $PM_{2.5}$ nmol/min·m^3. PM source apportionment was computed using the EPA PMF5.0 model and source contributions compared with those of a previous dataset collected between 2013 and 2014. Multi linear regression analysis identified which source contributed ($p<0.05$) to the oxidative potential of each size fraction. Inter-annual trends were more evident on $PM_{2.5}$ with reductions of biomass burning contribution and increases in traffic contribution in the 2016-2017 period. Crustal contributions were similar for the two periods, in both size fractions. Carbonates were comparable in PM_{10} with a slight increase in $PM_{2.5}$. Sea spray decreased in PM_{10}. The DTT_V of $PM_{2.5}$ peaked during cold periods, while, the DTT_V of the $PM_{10-2.5}$ fraction peaked in summer, suggesting that different sources, with different seasonality, influence OP in the $PM_{2.5}$ and $PM_{10-2.5}$ fractions. Analysis showed that sea spray, crustal, and carbonates sources contribute ~13.6% to DTT_V in $PM_{2.5}$ and ~62.4% to DTT_V in $PM_{10-2.5}$. Combustion sources (biomass burning and traffic) contribute to the majority of DTT_V (50.6%) in $PM_{2.5}$ and contribute for ~26% to DTT_V in $PM_{10-2.5}$. Secondary nitrate contributes to DTT_V in both fine and coarse fraction; secondary sulfate contribute to DTT_V in $PM_{2.5}$ with negligible contributions to DTT_V in $PM_{10-2.5}$.

Keywords: oxidative potential, source apportionment, PMF, PM composition trend, DTT assay

1. Introduction

Aerosol pollution represents a concern for environments, ecosystems, and human health. It has been associated with millions of premature deaths, cardiovascular and respiratory morbidity worldwide each year (Shiraiwa et al., 2017; Ahmed et al., 2018; Hallquist, et al., 2009; Lelieveld et al., 2015; Pope et al., 2015; Cohen et al., 2017). Atmospheric pollution affects not only developing countries but also Europe, the United States, and Australia, which, despite the progress made in reducing industrial and transport emissions, are still facing this problem.

Human exposure to high PM_{10} (where PM_{10} is referring to particles with an aerodynamic diameter < 10 μm) levels has been associated to different adverse health effects involving the cardiovascular and respiratory systems, diseases like lung cancer, and various kind of allergies (Manigrasso et al., 2022 and references therein). Prompted by the previous observations, in the 1997 the US EPA promulgated the NAAQS (National Ambient Air Quality Standards) for $PM_{2.5}$, adopting $PM_{2.5}$ as the indicator for fine particles (particles with an aerodynamic diameter < 2.5 μm) and identifying $PM_{2.5–10}$ as the coarse fraction of particles (i.e. particles having an aerodynamic diameter in the range 2.5-10 μm) (USEPA 2013). The coarse fraction, could have relevant health effects even it if is generally les studied compared to $PM_{2.5}$ (Adar et al., 2014). Roughly 4.2 million deaths were attributed to atmospheric pollution in 2016 by the World Health Organization (WHO). The majority of this mortality was due to exposure to fine particulate matter ($PM_{2.5}$). Lelieveld et al. (2019) reported, for Europe, an annual excess mortality rate of 659,000 cases due to air pollution, calculated for the year 2015, again largely attributable to $PM_{2.5}$. Furthermore, in Italy, the European Environment Agency (EEA, 2020) estimated that there were more than 50,000 premature deaths in 2018 attributable to long term exposure to $PM_{2.5}$. The new air quality guidelines of the WHO reduced the annual limit of $PM_{2.5}$ from 10 $\mu g/m^3$ to 5 $\mu g/m^3$ (WHO, 2021). The toxicity of PM depends on several physical and chemical properties, most of them related to their sources, nevertheless, the effective mechanisms driving toxicity are not yet fully understood (Kelly et al., 2012; Kim et al., 2015; Rönkkö et al., 2021; Valavanidis et al., 2008; WHO, 2013). There are several evidences that some adverse health effects

could be driven by oxidative stress induced by exposure to PM (Ayres et al., 2008; Bates et al., 2019; Guo et al., 2020; Li et al., 2015). As a consequence, several studies investigated the contributions of sources to oxidative potential (OP) of PM, intended as an indirect metric of the ability of PM to induce Reactive Oxygen Species (ROS) in biological systems (Costabile et al., 2019; Guascito et al., 2021; Massimi et al., 2020; Weber et al., 2021). A recent paper (Daellenbach et al., 2020) showed that the contributions of sources to PM mass concentrations and to OP are significantly different, suggesting that mitigation strategies aimed at reducing PM concentration alone could be not efficient in reducing oxidative potential. As a consequence, even if the link between OP and biological outcomes is still uncertain (Øvrevik, 2019; Lionetto et al., 2019; 2021; Jiang et al., 2019), it would be advisable to implement reduction strategies aimed to specific sources rather than to the total PM mass concentration and to investigate the long term trends of both PM concentration and composition.

In Europe, the emissions of a number of toxic atmospheric pollutants have been reduced during the last decades, with the aim to reduce the harmful effects of air pollution, in accordance with the 2008 Directive on Ambient Air Quality and Cleaner Air for Europe and with the 2004 Directive on heavy metals and polycyclic aromatic hydrocarbons in ambient air. However, the assessment of the outcomes of these policies needs comprehensive studies of the impacts of natural and anthropogenic sources to the composition of the atmosphere. For this reason, long term measurements of particulate matter concentrations and chemical compositions are recommendable to obtain reliable assessments of the time trends allowing to estimate efficiency of the enforced mitigation strategies. Some studies have been done using both numerical models and long term ground level measurements in Europe (Waked et al., 2018; Yang et al., 2020) and in other areas of the World (Kyllönen et al., 2020; Jain et al., 2020; Friedman, 2020). Yang et al. (2020) used a global aerosol-climate model with an explicit source tagging approach (CAM5-EAST) to investigate source apportionment of PM in Europe between 1980 and 2018. They found a decrease of about 62% of total near surface sulphate, black carbon, and primary organic carbon due to the reductions of local emissions in Europe with an 8-9% contribution from the reductions in the Russia-Belarus-Ukraine area. In Italy, a slow reduction of

PM_{10} and NO_2 levels were observed. This reduction is due to the joint decrease of primary particulate emissions and of the main precursors of secondary particulate matter (i.e. nitrogen oxides, sulfur oxides, ammonia) observed with the use of natural gas replacing fuels such as coal and oil, the introduction of catalysts in vehicles, and the adoption of technologies aimed at improving combustion processes in industrial processes. However, exceedances of the PM_{10} daily limit still occur in many urban areas and in monitoring stations located near important road arteries (ISPRA, 2017).

In the scientific literature, many studies aimed to characterize PM properties "in situ" based on PM measurements. However, most of these studies were based on sampling campaigns that lasted from weeks to months, whereas long-term (several years or multi-decadal) measurements of PM properties were done only in a limited number of sites (Rodríguez et al., 2012 and references therein). Long term measurements are crucial for many reasons, such as, the assessment of the consistency of remote sensing data (Chiapello et al., 1999; Smirnov et al., 2000); for model validations (Ginoux et al., 2004; Huneeus et al., 2010); for identification of processes affecting the evolution of dust emissions and transport (Prospero and Lamb, 2003).

The aims of this study are: (i) to investigate the inter-annual variability of the chemical composition of $PM_{2.5}$ and PM_{10}; (ii) using the positive matrix factorization model (PMF) to investigate the inter-annual trend of the contribution of the main natural and anthropogenic sources to the different PM fractions: $PM_{2.5}$, PM_{10} and the coarse $PM_{10-2.5}$; (iii) to evaluate the contributions of the different sources to the oxidative potential of PM in three size ranges, estimated using the DTT (Dithiothreitol) acellular assay. Particularly, only the PM water-soluble extract was analysed in term of OP (via DTT assay). This choice depends on observation that most of the literature OP data refers to the PM water-soluble fraction, that is considered more bioavailable (Gao et al., 2020a; Mukhtar et al., 2013). For example, many toxicological studies indicated the water-soluble metal as a possible harmful component of PM (Costa et al., 1997; Heal et al., 2005; Adamson et al., 2000; Ghio et al., 2001), showing that water-soluble metals were able to generate reactive oxygen species (ROS), which switch on cellular pro-inflammatory response pathways in vitro and in vivo (Mukhtar et al., 2013).

About the application of the OP assays to insoluble PM, this is very difficult and it is still not clear how much insoluble PM may contribute to the OP (Frezzini et al., 2022).

These aspects have been investigated using samples collected at an urban background Mediterranean site: the Environmental-Climate Observatory (ECO) of Lecce (South Italy). This observatory is a regional station of the Global Atmosphere Watch program (GAW-WMO) and a facility of the ACTRIS network, operative since 2013 (Dinoi et al., 2020; 2021a; 2021b; Cesari et al., 2018a; 2018b). Results provide data valuable for planning future mitigation strategies to reduce the impact of atmospheric particulate matter on health in this area.

2. Method

2.1. Measurement station and sampling

PM_{10} and $PM_{2.5}$ daily samples were collected at the Environmental-Climate Observatory (ECO) located inside the University Campus of Lecce (south Italy, 40°20'8''N– 18°07'28i''E, 37 m a.s.l., Figure S1). This Observatory is a regional station of the GAW- WMO network (Global Atmosphere Watch) and has been already deeply described in other works (Cesari et al., 2018a, 2018b; Dinoi et al., 2017).

Between 15/11/2016 and 17/11/2017, daily samples were continuously collected at the Observatory. Roughly, one sample every 3 days, for a total of 248 simultaneous samples (124 for PM_{10} and 124 for $PM_{2.5}$), was selected and analysed for this work. The sampler used was a low-volume (2.3 m^3/h) dual channel sequential sampler (SWAM, Fai Instruments srl, Italy). The instrument measures $PM_{2.5}$ and PM_{10} concentrations using an automatic detection based on β-ray attenuation with a typical uncertainty of 2% (PM_{10}) and 3% ($PM_{2.5}$) (Conte et al., 2020). Aerosol mass was collected on quartz filters (Whatman Q-grade, diameter 47 mm) thermally pre-treated at 700 °C for 2 hours.

2.2. Chemical analysis

The same approach of Cesari et al. (2018b) was used and it is here briefly described. Each filter was divided into four quarters, three of them used for the chemical analysis and one used for replication when needed.

A punch (1 cm^2) of one quarter of filter was used for determination of OC and EC using the thermo-optical transmittance (TOT) method (Sunset OC-EC Analyser), applying the EUSAAR2 protocol. The instruments was calibrated in the range 0-45 $\mu gC/cm^2$ using a sucrose standard solution. The LODs (Limit Of Detections) were 0.03 $\mu g/m^3$ (EC) and 0.1 $\mu g/m^3$ (OC) and typical measurement uncertainties were 5% for OC and 10% for EC (Merico et al., 2019). OC and EC concentrations were determined subtracting contamination on blank filters.

The second quarter of filter was used to extract the water-soluble fraction to be devoted both to oxidative potential analysis and concentrations of water soluble ions determination. The water-soluble fraction of collected PM was extracted in 15 mL of deionized water (Milli-Q 18 M Ω) using a 30-min sonication. A portion of each extract was used in High Performance Ion Chromatography (Dionex DX120 IC) system for determination of concentrations of major ions. The HPIC was equipped with an ED50 Conductivity detector, used with a 25 µL injection loop. Anions (Cl^- NO_3^-, SO_4^{2-}) were separated with a Dionex AS4A-4 column coupled with an IonPac AG14 guard column using as eluent 2.7 mM Na_2CO_3 and 1.0 mM $NaHCO_3$ in isocratic mode. Cations (Na^+, NH_4^+, K^+, Mg^{2+}, Ca^{2+}) were separated with a Dionex CS12A-4 column with IonPac CG12A guard column, using 20 mM MSA (methanesulfonic acid) as eluent in isocratic mode. The self-regenerating suppressors Dionex ASRS 300 for anions and Dionex CSRS 300 for cations were used. HPIC calibration was done using single anions and cations solutions (Thermo Scientific_Dionex_IC Standard). The method detection limits (MDLs) values (g/L) were as follows: 8.5 (Na^+), 7.0 (K^+), 45.2 (NH_4^+), 9.2 (Ca^{2+}), 2.5 (Mg^{2+}), 4.9 (Cl^-), 10.5 (NO_3^-), and 52 (SO_4^{2-}).

Another portion of the water-soluble extracts was filtered with PTFE syringe filters (0.45 µm porosity) to remove residual fibers and eventual insoluble materials. Successively, the filtered aliquots were used to evaluate the oxidative potential (DTT assay) following the methodology of Cho

et al. (2005). Specifically, 3.5 mL of each extract was incubated at 37 ° C adding 0.5 mL of DTT (1mM) and 1 mL of 0.5 M potassium phosphate buffer at pH 7.4 for times ranging from 5 to 90 minutes. At specific intervals (from 5 to 90 min), a 0.5 mL aliquot of the incubation mixture was collected and 0.5 mL of trichloroacetic acid (10% w/v) was added to stop the reaction. Afterwards, 2 mL of 0.4M Tris-HCl, pH 8.9 containing 20 mM EDTA and 25 μL of 10 mM DTNB was added and, after 1 minute the absorbance of the solution was measured, at 412 nm, using a UV-Vis UVIKON 942 (KONTRON) spectrophotometer. The DTT depletion rate (δ_{DTT}, pmol/min) was determined by linear regression between the measured absorbance and the time (Chirizzi et al., 2017). The detected values of δ_{DTT} were corrected using field blank measurements. The uncertainty on δ_{DTT}, determined by replication of measurements, was generally in the interval 3% - 15% (average ~ 6%). The DTT depletion rate allows to calculate the OP in terms of DTT_V, i.e. activity normalized with the air volume (V) actually sampled on each filter, or normalized with the mass of particulate matter collected on the filter DTT_M.

The third quarter of filter was used in ICP-MS (NexIon 300X, Perkin Elmer, USA) to determine concentration of different metals. Each sample was digested in closed Teflon vessels by a microwave digestor (Microwave Digestion System Start D, Milestone, Italy). The two steps procedure (EN 14385) was used. Firstly digestion in 1.2 mL HF (hydrofluoric acid, UltraTrace Analysis, 47%, Honeywell Fluka™) plus 1.8 mL HNO_3 (UltraTrace Analysis, 65-71%, Honeywell Fluka™) using temperature steps: from room temperature to 200 °C in 15 min, 15 min plateau at 200°C, and a final cooling back to room temperature. Successively, after addition of 14 mL of saturated H_3BO_3 (Sigma Aldrich, ACS reagent, ≥99.5%), temperature was increased to 200 °C in 10 min, a 15 min plateau followed, and a final cooling to room temperature. Finally, samples were diluted to 25 mL in volumetric flask using deionized water (Milli-Q® 18.2 MΩ). Each sample (1 mL) was transferred into 10 mL volumetric flask, Rh (Fluka, Spectroscopic Grade) (final concentration 5 μg/L) as internal standard and Y (Fluka, Spectroscopic Grade) (final concentration 5 μg/L - Indium in case of rare

earth elements analysis-) as second control were added and make up to the mark with 2% HNO_3 solution. The ICP-MS was tuned using a Multi-Element Standard for Instrument Calibration solution (Perkin Elmer) at 1 μg/L: Be, Ce, Fe, ln, Li, Mg, Pb, U. The external calibration was performed for the following elements: Al, As, Ba, Cd, Ce, Co, Cu, Dy, Fe, La, Li, Mn, Nd, Pb, Sb, Sr, Th, Ti, V, Zn using rare earth elements mix (Perkin Elmer) and single analyte standard solutions (Fluka, Spectroscopic Grade). Quality control checks were performed monitoring the intensities of all internal standards for every sample analysis and analyzing the laboratory control samples (LCS), in each sample batch, at a frequency of one LCS every 10 samples. The LCS were pre-fired quartz filters digested using the same procedure used for samples and a mix of standards, selected to control both matrix effect and possible memory effect. The MDLs, calculated with the same approach used for anions and cations, were between 0.007 μg/L (La) and 1.3 μg/L (Al).

Final concentrations of the different chemical species were corrected using the average level found in the blank samples. The concentration of a specific species in a samples was substituted with the threshold value $\sigma_B/2$ (i.e. one half of the standard deviation in blank filters) when it was too low to be quantified. Uncertainties for measured concentrations were evaluated as described in Cesari et al. (2018b).

2.3. Source apportionment using Positive Matrix Factorization

The EPA PMF5 receptor model was used to identify the number of sources, their chemical profiles, and their contributions to the measured $PM_{2.5}$ and PM_{10} concentrations. PMF is widely used worldwide for source apportionment being able to provide chemical profiles and contributions of sources, thereby operating with minimal information on the effective sources insisting on the site (Belis et al., 2020; Hopke et al., 2020). A single input data set was used, pooling together the chemical composition of $PM_{2.5}$ and PM_{10} fractions to improve robustness of the results. The input variables were classified using both, the Signal-to-Noise (S/N) criteria (Paatero and Hopke, 2003) and the percentage of data above the detection limits (Amato et al., 2016; Contini et al., 2016). The species

OC, EC, Cl, SO_4^{2-}, NH_4^+, K^+, Mg^{2+}, Ca^{2+}, Mn, Fe, As, and Ba, were classified as "strong" and used directly in PMF5; while, the species NO_3^-, Na^+, Al, V, Co, Cu, Zn, Sr, Sb, Dy, La, Nd, and Th were "weak". The best solution for the base run was obtained using seven factors: biomass burning, ammonium nitrate, traffic, sulphate, sea spray, crustal, and carbonates. Compared to the previous dataset, only the industrial source is missing likely because Pb (one of its main markers) was not available in the "2016-2017" dataset. Successively, a constrained run was performed in order to improve the separation between factors profiles (Amato et al., 2016; Cesari et al., 2021). The constraints used were: pull down maximally OC in traffic factor; pull up maximally SO_4^{2-} and Mg in crustal factor profile; pull down maximally OC in carbonate factor; pull up maximally NH_4^+ in secondary sulphate factor. The final dQ change, compared to the base run, was 7.8%. Uncertainty estimates in PMF results were obtained with the bootstrap method (Paatero et al., 2014). The bootstrap of the "constrained solution" (applied with 100 runs with random seed, block size suggested 23, and R=0.6) gave a good mapping of the solution with unmapped cases limited to 1% and 2% for traffic and nitrate (respectively) and to 6% (crustal) and 4% (carbonates).

Successively, a multi-linear regression (MLR) analysis was done between the daily contributions of the different sources estimated by the model PMF and the daily measured DTT_V values. This allowed to determine the contribution of each source identified by the PMF to the measured PM oxidative potential. The MLR was done using the XLSTAT tool imposing the intercept equal to zero and maintaining sources with statistical significance at 5% level (i.e. $p<0.05$). The approach is the same already used in a previous work (Cesari et al., 2019).

Finally, the differences observed between the seasonal periods considered (2013-2014 and 2016-2017) in terms of PM source contributions estimated by PMF and by stoichiometric calculations were performed using the Analysis Tool Pack of Microsoft Excel. The ANOVA (Analysis of Variance) test was used to test the significance of the differences observed and the threshold of the p-value was set at 5% (p-value 0.05) for the statistical test. All the significative differences founded with this test were shown with an asterisk in the figures reported in the results.

3. Results and discussion

3.1. Inter-annual variabilities of the different chemical species

Average (±standard deviations) concentrations of PM, elements, water soluble ions, and carbonaceous species detected in the period 2016-2017 are reported in Table S1 and compared with the results found in the previous dataset (collected in the period 2013-2014). The yearly average concentration was 18.0 (±11.4 standard deviation) μg/m^3 for the fine fraction ($PM_{2.5}$) and 26.9 (±12.7 standard deviation) μg/m^3 for the PM_{10} fraction. These values were comparable with the previous ones. The different measured species represent, on average, similar fractions of PM in the two periods: 55% of PM_{10} in 2016-2017 and 54% in 2013-24014; 60% of $PM_{2.5}$ in both measurement periods, 2016-2017 and 2013-2014.

The main components of PM are compared in Table S1 showing that the sums of metals were comparable in the two periods representing roughly 2-2.5% of PM in both size fractions. The sums of ions were slightly lower in the new dataset: 28.6% in 2016-2017 and 29.5% in 2013-2014 for PM_{10}; 26.7% in 2016-2017 and 27.8% in 2013-2014 for $PM_{2.5}$. Total carbon TC=OC+EC was comparable in the two measurement periods (for both size fractions), however, in 2016-2017 there was a slight shift with lower OC and larger EC compared to the previous period, even if considering the standard deviations, these differences were not statistically significant.

The analysis of the trends of the different chemical species (considering their averages and standard errors for the two period considered) showed comparable values of K^+ ion, often associated to biomass burning emissions. The same happened for the ions Na^+, Cl^- and Mg^{2+}, commonly considered of marine origin that could be a relevant source in this area (Contini et al., 2010). The slightly lower Cl^- observed in PM_{10} for the first period could be due to a different chlorine depletion in sea spray that is a relevant process observed at this site (Contini et al., 2014). The species associated to the secondary inorganic aerosol, NH_4^+, SO_4^{2-} and NO_3^-, showed different trends in the two

fractions: NH_4^+ showed a strong reduction in the second period of measurements (2016-2017) in both fractions, contrarily, SO_4^{2-} showed a limited reduction. Finally, NO_3^- showed an increase in both size fractions during the second measurement period. This could be interpreted with an increase of ammonium nitrate limited to $PM_{2.5}$, because nitrate in PM_{10}, at this site, is mainly due to sodium nitrate (Cesari et al., 2018b). The small reduction in secondary sulphate could be driven by the more limited availability of ammonium. Elements of crustal origin, particularly Al and Fe showed no trends, having similar concentrations during the two periods in both size fractions. Ca^{2+}, that at this site is mainly related to carbonates due to re-suspended soil (Contini et al., 2014), was comparable in PM_{10} but presented an increase in $PM_{2.5}$ during the 2016-2017 period. V, Co, and As had larger concentrations in the 2016-2017 period and also larger standard deviations, however, the median values were comparable in the two measurement periods. Dy showed larger concentrations in the 2016-2017 period. All the other elements detected in both fractions showed comparable concentrations in the two sampling periods.

Mass closure approach and OC/EC ratio have been used to evaluate yearly variabilities of secondary organic and inorganic aerosol, marine and crustal contributions to PM mass collected. The OC/EC minimum ratio method was used to estimate the secondary organic carbon (SOC) concentrations applying the equation reported in Pio et al., (2011), based on the $(OC/EC)_{min}$. This average ratio was 5.9 (±2.4) in PM_{10} and 5.2 (±2.0) in $PM_{2.5}$, in reasonable agreement with the ratios observed in the first period of measurements (2013-2014) within the uncertainty intervals, that were 7.8 (±3.9) in PM_{10} and 8.8 (±4.9) in $PM_{2.5}$ (Cesari et al., 2018b). As stated in Cesari et al. (2018b, and references therein), the large OC/EC values observed were compatible with an urban background site mainly influenced by biomass burning. The $(OC/EC)_{min}$ ratios were determined separately for PM_{10} and $PM_{2.5}$, looking at the minimum slopes, that was equal to 2 for both fractions (Figure S2). By calculations, SOC was 3.28 $\mu g/m^3$ representing 62% of total OC in PM_{10}, and 2.70 $\mu g/m^3$ representing 56% of total OC in $PM_{2.5}$. The non-sea-salt sulphate was evaluated as nss-SO_4^{2-} = SO_4^{2-} - 0.25Na^+, and represented 91% of total sulphate in PM_{10} and 97% in $PM_{2.5}$. The correlation between

SO_4^{2-} and NH_4^+, 0.55 ($p < 0.05$) and 0.61 ($p < 0.05$) for PM_{10} and $PM_{2.5}$, respectively, indicated likely the presence of a certain amount of ammonium sulphate in the sampled PM, estimated as 2.6 (± 1.6) μg/m^3 in PM_{10} and 2.5 (± 1.4) μg/m^3 in $PM_{2.5}$. The correlations between ion Na^+ with Cl^- and with Mg^{2+}, respectively 0.61 and 0.66, typically indicates the presence of sea spray (Querol et al., 2001). This contribution was evaluated as Cl^- + 1.4468 * Na^+ (Marenco et al., 2006) and was 2.1 (± 1.8) μg/m^3 for PM_{10} and 0.6 (± 0.4) μg/m^3 for $PM_{2.5}$, with a major concentration in PM_{10} fraction as expected. The crustal contribution was calculated using the formula 1.15(1.89Al + 2.14Si + 1.67Ti + 1.4Ca* + 1.2K* + 1.36 Fe) that consider metal oxides of Al, Si and Fe, plus the insoluble fraction of K and Ca indicated with an asterisk (Cesari et al., 2018b). Carbonates were calculated from non-sea-salt calcium and magnesium as 1.5 nss-Ca^{2+} + 2.5 nss-Mg^{2+} (Perrino et al., 2014). The crustal contribution, together with the carbonates, were 3.25 (± 3.32) μg/m^3 and 2.14 (± 1.84) μg/m^3 respectively for PM_{10}, while in $PM_{2.5}$ were 1.87 (± 2.15) μg/m^3 and 1.06 (± 1.19) μg/m^3.

Figure 1 shows the average concentrations of secondary organic carbon (SOC), secondary inorganic aerosol (SIA, sum of nitrate, ammonium, and sulphate), sea spray, crustal, and carbonates in absolute and relative terms, for the two sampling periods and for the two fractions PM_{10} and $PM_{2.5}$. Considering the PM_{10} fraction, while contributions of natural origin, sea spray, crustal and carbonate were similar, within the uncertainty ranges, a difference, even if not significative, was observed for secondary organic and inorganic aerosol contributions, with a decreasing trend for both of them. These differences could be mainly due to different atmospheric conditions (such as temperature, relative humidity, presence of precursors) that could lead to different concentrations of secondary aerosols in air. Looking at the $PM_{2.5}$ fraction, marine and crustal sources provided similar concentrations in the two period and a decrease of SOC and SIA was observed as in PM_{10} but is statistical significative only for SOC. Carbonates showed a significative difference, with an increasing trend compatible with the large Ca^{2+} concentrations observed in 2016-2017 limited to $PM_{2.5}$.

3.2. Trends of the contributions of sources

The best PMF5 solution was obtained using seven factors that were similar to those previously identified in Cesari et al. (2018b). The source profiles were shown in Figure 2. PMF5 reconstructed reasonably well measured concentrations for both size fractions (Fig. 2h). The portion unexplained by the model (i.e. the average difference between measured and reconstructed concentrations) was +6% for PM_{10} and -6% for $PM_{2.5}$. The linear fit of the correlation between measured and reconstructed PM concentrations had a slope of 1.06 (±0.02), an intercept of -1.1 (±0.6) $\mu g/m^3$ and a determination coefficient R^2 of 0.89.

Figure 3 reports the estimated contributions, in absolute and relative terms, for the factors/sources identified and a comparison with the previous results obtained for the 2013-2014 period. In addition, Fig. 3 includes the sources evaluated with the calculations based on measured concentrations (Section 4.1 and indicated as “mass closure” values). As showed in Fig. 3, the differences observed are statistically significative only for $PM_{2.5}$ fraction (i.e. secondary nitrate, traffic, secondary sulphate and carbonates). There was a small reduction of biomass burning contribution, more evident on $PM_{2.5}$ with respect to PM_{10} and an increase of the traffic contribution, again more relevant for $PM_{2.5}$. It is noteworthy that the sum of these two main combustion sources was essentially constant in the two measurement periods and for the two size fractions. This could indicate a difficulty in separating the contributions of these two sources in the PMF source apportionment approach (Cesari et al., 2021). Crustal contributions were similar for the two periods and in the two size fractions, while, carbonates were comparable in PM_{10} but a slight increase was observed in $PM_{2.5}$ in agreement with the increase of concentrations of Ca^{2+} observed in this size fraction (Section 4.1). Sea spray decreased in PM_{10} but not in $PM_{2.5}$. This difference was probably due to the variability of atmospheric conditions, i.e. wind intensity and direction that could affect strongly sea spray generation and transport at this site (Contini et al., 2010). Secondary nitrate in the two measurement periods was comparable in PM_{10} but an increase was observed in the fine fraction

($PM_{2.5}$) together with a decrease of secondary sulphate. This is compatible with a partial shift from ammonium sulphate to ammonium nitrate in 2016-2017, as it was hypothesized in Section 4. This shift involving ammonium is more relevant in $PM_{2.5}$ because a previous study at this site (Cesari et al., 2018b) showed that nitrate in fine fraction is mainly ammonium nitrate especially in the cold periods, while sodium nitrate is the most relevant form of nitrate for the coarse fraction ($PM_{10-2.5}$). It is interesting to observe that SIA (sum of secondary nitrate and sulphate) was essentially constant in the two periods and in the two size fractions, within the variabilities indicated in Fig. 3.

The comparison of PMF contributions with the calculations based on measured concentrations (mass closure on Fig. 3) were in reasonable agreement for sea spray, crustal, and carbonates; however, there was an overestimation of SIA using PMF. This suggests that the chemical profiles of secondary sources obtained by PMF were not purely stoichiometric nitrate and sulphate. This difference was observed also in other sites in central Italy (Cesari et al., 2016) and it can be particularly relevant for the contribution of secondary nitrate.

3.3. Influence of chemical composition and sources on oxidative potential

In Table S2, the yearly average of DTT_V and DTT_M detected in PM_{10} and $PM_{2.5}$ were compared with values measured in other urban background sampling sites of Italy and Europe. The values observed at the site studied were comparable, within the variability range, with the levels observed in the other sites.

Figure 4a shows the yearly and seasonal averages of DTT_V in the $PM_{2.5}$ and in the coarse fraction. The lower values of DTT_V observed in the coarse fraction, compared to that of fine PM fraction, were compatible with results discussed in other studies (Massimi et al., 2020; Paraskevopoulou, et al. 2019; Simonetti et al., 2018). DTT_V of $PM_{2.5}$ peaked during the cold period, likely as a consequence of higher combustion emissions and of shallower boundary layer height that concentrates ground-level aerosol, suggesting a possible association of OP with local winter sources (such as biomass burning and traffic). DTT_V in the $PM_{10-2.5}$ fraction followed a different seasonal

trend with the largest average value observed in summer suggesting that different sources influenced OP in the two size fractions. This was confirmed by an analysis of Pearson correlation coefficients because DTT_V in $PM_{2.5}$ had relevant ($p<0.05$) correlations with the species OC (Pearson 0.69), EC (0.69), NO_3^- (0.46), and K^+ (0.62) that are commonly associated to combustions sources emissions (Matawle et al., 2015; Callén et al., 2013). While, negligible correlations were observed with soil and crustal elements. DTT_V in the coarse fraction had lower correlation coefficients, compared to $PM_{2.5}$, with OC and EC (~0.3) and larger coefficients, again in comparison with $PM_{2.5}$, for crustal and soil elements Al, Fe, Ca^{2+} (between 0.2 and 0.4).

Figure 4b shows the yearly and seasonal values of the specific oxidative potential (i.e. DTT_M) for $PM_{2.5}$, PM_{10}, and $PM_{10-2.5}$. The DTT_M had a seasonal trend similar to that of DTT_V peaking during the cold period (winter and autumn). The DTT_M of the coarse fraction was quite relevant, being about 70% (on average) of that calculated for $PM_{2.5}$, even if the DTT_V was about 2.9-time lower than that observed on $PM_{2.5}$. This was compatible with the results obtained in other sites (Hu et al., 2008). Considering studies on PM oxidative DTT potential trends reported in literature, are evident the high differences in OP trends detected in different sampling sites around the world. For example, in Nanjing (Yang et al., 2021) no obvious seasonal difference of OP_V was observed for outdoor $PM_{2.5}$, while the outdoor OP_M exhibited a significant seasonal variation, with higher values in autumns and summer and the lowest in winter (Yang et al., 2021). In Hong Kong (Cheng et al., 2021) the OP trend was clearly correlated to meteorological conditions, being higher on regional days than on LRT and local days. Where the sampling days were classified into three categories mainly based the air mass backward trajectories, which are regional days (air quality in Hong Kong mainly influenced by continental air masses from the Pearl River Delta (PRD) region), long-range transport (LRT) days (mainly affected by northeastern coastal air masses), and local days (mainly under influence of local emission sources). Conversely, in another study performed in Atlanta (Gao et al., 2020b) there was no significant seasonal variation observed for either volume or mass- normalized OP water soluble DTT. In contrast, both volume and mass-normalized OPtotal- DTT and thus OP water insoluble- DTT

varied between seasons, with higher levels in the cold months (Jan–Mar, Dec) than in summer (Jun–Aug).

The contributions to OP of the PM sources identified were estimated using the MLR approach, assuming that the DTT_V was a linear combination of the PM mass concentrations due to the different sources obtained with PMF5 (Weber et al., 2018). The slopes (i.e. fitting coefficients) represent the intrinsic contributions of each source (expressed as nmol/min·μg). MLR results had $R^2 = 0.88$ (R^2 correct = 0.87) and a RMSE (root mean standard error) equal to 0.14. The model gave a reasonable fit of the variables considered, as shown in Fig. 5(c). Table S3 reports the results of MLR analysis, in terms of intrinsic contributions, standard error, p-values at 95% confidence intervals showing, for each source investigated, that the MLR model gave a good fit for all sources.

Figure 5 shows the contributions, in absolute and in relative terms, of the different sources to DTT_V activity. MLR results showed that the different sources contribute differently to DTT_V in fine and coarse fraction confirming the hypothesis obtained by the analysis of the seasonal trends and correlations. Sea spray, crustal, and carbonates, that are mainly sources of natural and soil origin at this site (Cesari et al., 2018; Contini et al., 2014) had a small relative contribution (~13.6% in total) to DTT_V in $PM_{2.5}$ but they represented the majority of the contribution (~62.4% in total) of DTT_V in the coarse fraction. Contrarily, the main combustion sources (biomass burning and traffic) contributed to the majority of DTT_V (about 50.6%) in $PM_{2.5}$ but contributed for only ~26% to DTT_V in the coarse fraction. The low contribution of natural sources to DTT_V compared to combustion sources in $PM_{2.5}$ or in PM_{10} was compatible with the results of other studies (Liu et al., 2018; Cesari et al., 2019; Paraskevopoulou et al., 2019). Secondary nitrate contributed to DTT_V in both fine and coarse fractions, while secondary sulphate contributed to DTT_V in $PM_{2.5}$ but had a negligible contribution to $DTTT_V$ in the $PM_{10\text{-}2.5}$ fraction. The contribution of nitrate was observed also in other studies (Cesari et al., 2019; Paraskevopoulou et al., 2019) and it is likely due to the combustion origin of nitrate precursors, for example from traffic and biomass burning. The MLR analysis showed also high contributions to DTT_V from secondary sulphate. Ammonium sulphate is not considered as a

strong redox agent and in some works (Cesari et al., 2019; Fang et al., 2016) secondary sulphate gave an insignificant contribution to DTT_V. However, in other studies a relevant contribution of secondary sulphate to DTT_V was observed (Liu et al., 2018; Massimi et al., 2020; Paraskevopoulou et al., 2019). Results of this work showed a contribution from secondary sulphate to DTT_V in $PM_{2.5}$ but a negligible contribution to DTT_V in $PM_{10\text{-}2.5}$. This could be due to the presence of a certain amount of secondary organic sulphate, in this source profile, that could influence and increase the measured DTT activity of this source (Hakimzadeh et al., 2020; Verma et al., 2015).

4. Conclusions

This research aimed to connect specific sources of PM to changes in seasons, as well as possible adverse health outcomes. The inter-annual trends of the contributions of the main sources to $PM_{2.5}$ and PM_{10} and to their oxidative potential (in terms of DTT_V) were assessed at the Environmental-Climate Observatory (ECO) of Lecce (South Italy).

Results showed comparable values of total carbon for both $PM_{2.5}$ and PM_{10}, with a decrease of OC and an increase of EC. Comparable values in the two periods were observed for ions K^+, Na^+, Cl^- and Mg^{2+}. Between 2013 and 2017, an increase of ammonium nitrate and a small decrease of ammonium sulphate in $PM_{2.5}$ was observed. However, the total SIA was essentially constant in both $PM_{2.5}$ and PM_{10}. Elements of crustal origin Al, Fe showed no trends, but there was an increase of Ca^{2+} only in $PM_{2.5}$.

Results of source apportionment showed that from 2013 to 2017 there is a reduction of the biomass burning contribution and an increase of traffic contribution. This was more relevant for $PM_{2.5}$ compared to PM_{10}. However, the sums of these two main combustion sources were comparable in the two periods. This could indicate a difficulty in separating the contributions of these two sources in the application of PMF5. Crustal contributions were similar for the two periods in both $PM_{2.5}$ and PM_{10}, while carbonates were comparable in PM_{10} but a slight increase was observed in $PM_{2.5}$. Sea spray decreased in PM_{10}, likely because of the variability of atmospheric conditions.

The DTT_V of $PM_{2.5}$ peaked during the cold period, as a consequence of higher contributions of combustion sources. The DTT_V in the $PM_{10-2.5}$ fraction followed a different seasonal trend with maximum average value observed in summer, suggesting that different sources, having different seasonality, influenced OP in these two size fractions. The DTT_V of $PM_{10-2.5}$ was, on average, significantly lower than that of $PM_{2.5}$. The MLR analysis of sources contributing to DTT_V showed that natural sources (i.e. sea spray, crustal and carbonates) have a small relative contribution (~13.6% in total) to DTT_V in $PM_{2.5}$ but they represented the major contributors (~62.4% in total) to DTT_V in the $PM_{10-2.5}$ fraction. Conversely, combustion sources (biomass burning and traffic) contributed to the majority of DTT_V (about 50.6%) in $PM_{2.5}$ but contribute for only ~26% to DTT_V in the $PM_{10-2.5}$ fraction. Secondary nitrate contributed to DTT_V in both size fractions, while secondary sulphate contributed to DTT_V in $PM_{2.5}$ with a negligible contribution to DTT_V in the $PM_{10-2.5}$ fraction.

The results could be extended in future studies to investigate trends on longer periods and could provide valuable information for planning future mitigation strategies aimed to reduce the impact of atmospheric particulate matter on health in this area.

Acknowledgements

This work was supported by I-AMICA (Infrastructure of High Technology for Environmental and Climate Monitoring - PONa3_00363), a project of structural improvement financed under the National Operational Program (NOP) for “Research and Competitiveness 2007–2013” co-funded with European Regional Development Fund (ERDF) and National resources. Additional support of the project CIR01_00015 - PER-ACTRIS-IT “Potenziamento della componente italiana della Infrastruttura di Ricerca Aerosol, Clouds and Trace Gases Research Infrastructure - Rafforzamento del capitale umano” - Avviso MUR D.D. n. 2595 del 24.12.2019 Piano Stralcio “Ricerca e Innovazione 2015-2017” is gratefully acknowledged.

Declaration of interests

The authors declare that they have no known competing interests.

Author contributions.

D. Contini, M.R. Guascito, A. Mangone conceptualized the study design; A. Dinoi and E. Merico collected the samples and performed analysis of carbon content; A. Mangone and L.C. Giannossa performed chemical analysis. D. Cesari and D. Contini did statistical analysis and prepared the draft. All authors collaborated to interpretation of results, wrote, read, commented, and approved the final manuscript.

References

Adamson, I.Y.R., Prieditis, H., Hedgecock C., Vincent, R., 2000. Zinc is the toxic factor in the lung response to an atmospheric particulate sample. Toxicol. Appl. Pharmacol. 166, 111–119.

Adar, S.D., Filigrana, P.A., Clements, N., Peel, J.L., 2014. Ambient Coarse Particulate Matter and Human Health: A Systematic Review and Meta-Analysis. Curr. Environ. Health Rep. 1(3), 258-274.

Ahmed, C.M.S., Jiang, H., Chen, Y.J., Lin,Y.-H., 2018. Traffic-related particulate matter and cardiometabolic syndrome: a review. Atmosphere, 9.

Altuwayjiri, A., Pirhadi, M., Taghvaee, S., Sioutas, C., 2021. Long-term trends in the contribution of PM2. 5 sources to organic carbon (OC) in the Los Angeles basin and the effect of PM emission regulations. Faraday Discuss., 226, 74-99.

Amato, F., Alastuey, A., Karanasiou, A., Lucarelli, F., Nava, S., Calzolai, G., Severi, M., Becagli, S., Vorne, L.G., Colombi, C., Alves, C., Custódio, D., Nunes, T., Cerqueira, M., Pio, C., Eleftheriadis, K., Diapouli, E., Reche, C., Minguillón, M.C., Manousakas, M.I., Maggos, T., Vratolis, S., Harrison, R.M., Querol, X., 2016. AIRUSE-LIFEC: a harmonized PM speciation and source apportionment in five southern European cities. Atmos. Chem. Phys., 16, 3289-3309.

Ayres, J.G., Borm, P., Cassee, F.R., Castranova, V., Donaldson, K., Ghio, A., Harrison, R.M., Hider, R., Kelly, F., Kooter, I.M., Marano, F., Maynard, R.L., Mudway, I., Nel, A., Sioutas, C., Smith, S., Baeza-Squiban, A., Cho, A., Duggan, S., and Froines, J., 2008. Evaluating the Toxicity of Airborne Particulate Matter and Nanoparticles by Measuring Oxidative Stress Potential – A Workshop Report and Consensus Statement, Inhal. Toxicol., 20, 75–99.

Bates, J.T., Fang, T., Verma, V., Zeng, L., Weber, R.J., Tolbert, P.E., Abrams, J.Y., Sarnat, S.E., Klein, M., Mulholland, J.A., Russell, A.G., 2019. Review of acellular assays of ambient particulate matter oxidative potential: methods and relationships with composition, sources, and health effects. Environ. Sci. Technol. 53, 4003–4019.

Belis, C.A., Pernigotti, D., Pirovano, G., Favez, O., Jaffrezo, J.L., Kuenen, J., Denier van Der Gon, H., Reizer, M., Riffault, V., Alleman, L.Y., Almeida, M., Amato, F., Angyal, A., Argyropoulos, G., Bande, S., Beslic, I., Besombes, J.-L., Bove, M.C., Brotto, P., Calori, G., Cesari, D., Colombi, C., Contini, D., De Gennaro, G., Di Gilio, A., Diapouli, e., El Haddad, I., Elbern, H., Eleftheriadis, K., Ferreira, J., Garcia Vivanco, M., Gilardoni, S., Golly, B., Hellebust, S., Hopke, P.K., Izadmanesh, Y., Jorquera, H., Krajsek, K., Kranenburg, R., Lazzeri, P., Lenartz, L., Lucarelli, F., Maciejewska, K., Manders, A., Manousakas, M., Masiol, M., Mircea, M., Mooibroek, D., Nava, S., Oliveira, D., Paglione, M., Pandolfi, M., Perrone, M., Petralia, E., Pietrodangelo, A., Pillon, S., Pokorna, P., Prati, P., Salameh, D., Samara, C., Samek, L., Saraga, D., Sauvage, S., Schaap, M., Scotto, F., Sega, K., Siour, G., Tauler, R., Valli, G., Vecchi, R., Venturini, E., Vestenius, M., Waked, A., Yubero, E., 2020. Evaluation of receptor and chemical transport models for PM10 source apportionment. Atmos. Environ. X 5, 100053.

Callén, M.S., López, J.M., Mastral, A.M., 2013. Influence of organic and inorganic markers in the source apportionment of airborne PM10 in Zaragoza (Spain) by two receptor models. Environ. Sci. Poll. Res., 20, 3240–3251.

Cesari, D., Donateo, A., Conte, M., Contini, D., 2016. Inter-comparison of source apportionment of PM10 using PMF and CMB in three sites nearby an industrial area in central Italy. Atmos. Res., 182, 282–293.

Cesari, D., Merico, E., Dinoi, A., Marinoni, A., Bonasoni, P., Contini, D., 2018a. Seasonal variability of carbonaceous aerosols in an urban background area in Southern Italy. Atmos. Res., 200, 97-108.

Cesari, D., De Benedetto, G.E., Bonasoni, P., Busetto, M., Dinoi, A., Merico, E., Chirizzi, D., Cristofanelli, P., Donateo, A., Grasso, F.M., Marinoni, A., Pennetta, A., Contini, D., 2018b. Seasonal variability of PM2.5 and PM10 composition and sources in an urban background site in Southern Italy. Sci. Tot. Environ., 612, 202-213.

Cesari, D., Merico, E., Grasso, F.M., Decesari, S., Belosi, F., Manarini, F., De Nuntiis, P., Rinaldi, M., Volpi, F., Gambaro, A., Morabito, E., Contini D., 2019. Source Apportionment of PM2.5 and of its Oxidative Potential in an Industrial Suburban Site in South Italy. Atmosphere, 10, 12, 758.

Cesari, D., Merico, E., Grasso, F.M., Dinoi, A., Conte, M., Genga, A., Siciliano, M., Petralia E., Stracquadanio M., Contini D., 2021. Analysis of the contribution to PM10 concentrations of the largest coal-fired power plant of Italy in four different sites. Atmos. Poll. Res., 12, 8.

Cheng, Y, Ma, Y, Dong, B, Qiu, X, Hu, D, 2021. Pollutants from primary sources dominate the oxidative potential of water-soluble PM2.5 in Hong Kong in terms of dithiothreitol (DTT) consumption and hydroxyl radical production. J. Hazard. Mater., 405, 124218.

Chiapello, I., Prospero, J.M., Herman, J., Hsu, C., 1999. Detection of mineral dust over the North Atlantic Ocean and Africa with the Nimbus 7 TOMS. J. Geophys. Res., 104, 9277–9291.

Chirizzi, D., Cesari, D., Guascito, M.R., Dinoi, A., Giotta, L., Donateo, A., Contini, D., 2017. Influence of Saharan dust outbreaks and carbon content on oxidative potential of water-soluble fractions of $PM_{2.5}$ and PM_{10}. Atmos. Environ., 163, 1-8.

Cho, A.K., Sioutas, C., Miguel, A.H., Kumagai, Y., Schmitz, D.A., Singh, M., Eiguren-Fernandez, A., Froines, J.R., 2005. Redox activity of airborne particulate matter at different sites in the Los Angeles Basin. Environ. Res., 99, 40–47.

Cohen, A.J., Brauer, M., Burnett, R., Anderson, H.R., Frostad, J., Estep, K., Balakrishnan, K., Brunekreef, B., Dandona L., Dandona R., Feigin V., Freedman G., Hubbell B., Jobling A., Kan H., Knibbs L., Liu Y., Martin R., Morawska L., Pope C.A., Shin H., Straif K., Shaddick G., Thomas M., van Dingenen R., van Donkelaar A., Vos T., Murray C.J.L., Forouzanfaret M.H., 2017. Estimates and 25-year trends of the global burden of disease attributable to ambient air pollution: an analysis of data from the Global Burden of Diseases Study 2015. Lancet, 389, 1907–1918.

Costa, D.L., Dreher, K.L., 1997. Bioavailable transition metals in particulate matter mediate cardiopulmonary injury in healthy and compromised animal models. Environ. Health Perspect. 105, 1053–1060.

Contini, D., Genga, A., Cesari, D., Siciliano, M., Donateo, A., Bove, M.C., Guascito, M.R., 2010. Characterisation and source apportionment of PM10 in an urban background site in Lecce. Atmos. Res., 95, 1, 40-54.

Contini, D., Cesari, D., Genga, A., Siciliano, M., Ielpo, P., Guascito, M.R., Conte, M., 2014. Source apportionment of size-segregated atmospheric particles based on the major water-soluble components in Lecce (Italy). Sci. Total Environ., 472, 248–261.

Contini, D., Cesari, D., Conte, M., Donateo, A., 2016. Application of PMF and CMB receptor models for the evaluation of the contribution of a large coal-fired power plant to PM10 concentrations. Sci. Total Environ., 560–561, 131-140.

Conte, M., Merico, E., Cesari, D., Dinoi, A., Grasso, F.M., Donateo, A., Guascito, M.R., Contini, D., 2020. Long-term characterisation of African dust advection in south-eastern Italy: Influence on fine and coarse particle concentrations, size distributions, and carbon content, Atmos. Res., 233, 104690.

Costabile, F., Gualtieri, M., Canepari, S., Tranfo, G., Consales, C., Grollino, M.G., Paci E., Petralia E., Pigini D., Simonetti G., 2019. Evidence of association between aerosol properties and in-vitro cellular oxidative response to PM1, oxidative potential of PM2.5, a biomarker of RNA oxidation, and its dependency on combustion sources. Atmos. Environ., 213, 444–455.

Daellenbach, K.R., Uzu, G., Jiang, J., Cassagnes, L.-E., Leni, Z., Vlachou, A., Stefenelli, G., Canonaco, F., Weber, S., Segers, A., Kuenen, J.J.P., Schaap, M., Favez, O., Albinet, A., Aksovoglu, S., Dommen, J., Baltensperger, U., Geiser, M., El Haddad, I., Jaffrezo, J., Prévôt, A.S.H., 2020. Sources of particulate-matter air pollution and its oxidative potential in Europe. Nature, 587, 414–419.

Dinoi, A., Cesari, D., Marinoni, A., Bonasoni, P., Riccio, A., Chianese, E., Tirimberio, G., Naccarato, A., Sprovieri, F., Andreoli, V., Moretti, S., Gullì, D., Calidonna, C.R., Ammoscato, I., Contini, D., 2017. Inter-Comparison of Carbon Content in PM2.5 and PM10 Collected at Five Measurement Sites in Southern Italy. Atmosphere, 8, 12, 243.

Dinoi, A., Gulli, D., Ammoscato, I., Calidonna, C.R., Contini D., 2021a. Impact of the Coronavirus Pandemic Lockdown on Atmospheric Nanoparticle Concentrations in Two Sites of Southern Italy. Atmosphere, 12, 3, 352.

Dinoi, A., Weinhold, K., Wiedensohler, A., Contini, D., 2021b. Study of new particle formation events in southern Italy. Atmos. Environ., 244,117920.

EEA, 2020. Report No 09/2020 Air quality in Europe.

Fang, T., Verma, V., Bates, J.T., Abrams, J., Klein, M., Strickland, M.J., Sarnat, S.E., Chang, H.H., Mulholland, J.A., Tolbert, P.E., Russel, A.G., Weber, R.J., 2016. Oxidative potential of ambient water-soluble PM2.5 in the southeastern United States: Contrasts in sources and health associations between ascorbic acid (AA) and dithiothreitol (DTT) assays. Atmos. Chem. Phys., 16, 3865–3879.

Frezzini, M.A., Di Iulio, G., Tiraboschi, C., Canepari, S., Massimi, L. 2022A New Method for the Assessment of the Oxidative Potential of Both Water-Soluble and Insoluble PM. *Atmosphere* , *13*, 349.

Friedman, B., 2020. Source apportionment of PM2.5 at two Seattle chemical speciation sites. J. Air Waste Manag. Assoc., 70(7), 687-699.

Heal, M.R., Hibbs, L.R., Agius, R.M., Beverland, I.J., 2005. Total and water-soluble trace metal content of urban background PM10, PM2.5 and black smoke in Edinburgh, UK. Atmos. Environ. 39, 1417–1430.

ISPRA, 2017. Qualità dell'ambiente urbano – XIII Rapporto ISPRA Stato dell'Ambiente 74/17 ISBN 978-88-448-0858-7.

Gao, D.; Ripley, S.; Weichenthal, S.; Pollitt, K.J.G., 2020a. Ambient particulate matter oxidative potential: Chemical determinants, associated health effects, and strategies for risk management. Free Radic. Biol. Med., 151, 7–25.

Gao, D., Mulholland, J.A., Russell, A.G., Weber, R.J., 2020b. Characterization of water-insoluble oxidative potential of PM2.5 using the dithiothreitol assay. Atmos. Environ. 224, 117327.

Ghio, A.J., Devlin R.B., 2001. Inflammatory lung injury after bronchial instillation of air pollution particles. Am. J. Respir. Crit. Care Med. 164, 704–708.

Ginoux, P., Prospero, J.M., Torres, O., Chin, M., 2004. Long-term simulation of global dust distribution with the GOCART model: Correlation with North Atlantic Oscillation. Environ. Model. Softw., 19, 113–128.

Guascito, M.R., Pietrogrande, M.C., Decesari, S., Contini, D., 2021. Oxidative Potential of Atmospheric Aerosols. Atmosphere, 12 (5), 531.

Guo, H., Jin, L., and Huang, S., 2020. Effect of PM characterization on PM oxidative potential by acellular assays: a review. Rev. Environ. Health, 35, 4, 461-470.

Hakimzadeh, M., Soleimanian, E., Mousavi, A., Borgini, A., De Marco, C., Ruprecht, A.A., Sioutas, C., 2020. The impact of biomass burning on the oxidative potential of PM2.5 in the metropolitan area of Milan. Atmos. Environ., 224, 117328.

Hallquist, M., Wenger, J. C., Baltensperger, U., Rudich, Y., Simpson, D., Claeys, M., Dommen, J., Donahue, N. M., George, C., Goldstein, A. H., Hamilton, J. F., Herrmann, H., Hoffmann, T., Iinuma, Y., Jang, M., Jenkin, M. E., Jimenez, J. L., Kiendler-Scharr, A., Maenhaut, W., McFiggans, G.,

Mentel, Th. F., Monod, A., Prévôt, A. S. H., Seinfeld, J. H., Surratt, J. D., Szmigielski, R., and Wildt, J., 2009. The formation, properties and impact of secondary organic aerosol: current and emerging issues. Atmos. Chem. Phys., 9, 5155–5236.

Hopke, P.K., Dai, Q., Li, L., Feng, Y., 2020. Global review of recent source apportionments for airborne particulate matter. Sci. Total Environ. 740, 140091.

Hu, S., Polidori, A., Arhami, M., Shafer, M.M., Schauer, J.J., Cho, A., and Sioutas, C., 2008. Redox activity and chemical speciation of size fractioned PM in the communities of the Los Angeles-Long Beach harbor. Atmos. Chem. Phys., 8, 6439–6451.

Huneeus, N., Schulz, M., Balkanski, Y., Griesfeller, J., Prospero, J., Kinne, S., Bauer, S., Boucher, O., Chin, M., Dentener, F., Diehl, T., Easter, R., Fillmore, D., Ghan, S., Ginoux, P., Grini, A., Horowitz, L., Koch, D., Krol, M.C., Landing, W., Liu, X., Mahowald, N., Miller, R., Morcrette, J.-J., Myhre, G., Penner, J., Perlwitz, J., Stier, P., Takemura, T., Zender, C.S., 2010. Global dust model intercomparison in AeroCom phase I. Atmos. Chem. Phys., 11, 7781–7816.

Jain, S., Sharma, S.K., Vijayan, N., Mandal, T.K., 2020. Seasonal characteristics of aerosols (PM2.5 and PM10) and their source apportionment using PMF: A four year study over Delhi, India. Environ. Poll., 262, 114337.

Jedynska, A., Hoek, G., Wang, M., Yang, A., Eeftens, M., Cyrys, J., Keuken, M., Ampe, C., Beelen, R., Cesaroni, G., Forastiere, F., Cirach, M., de Hoogh, K., De Nazelle, A., Nystad, W., Akhlaghi, H.M., Declercq, C., Stempfelet, M., Eriksen, K.T., Dimakopoulou, K., Lanki, T., Meliefste, K., Nieuwenhuijsen, M., Yli-Tuomi, T., Raaschou-Nielsen, O., Janssen, N.A.H., Brunekreef, B., Kooter, I.M., 2017. Spatial variations and development of land use regression models of oxidative potential in ten European study areas. Atmos. Environ. 150, 24-32.

Jiang, H., Ahmed, C.M.S., Canchola, A., Chen, J.Y., Lin, Y-H., 2019. Use of Dithiothreitol Assay to Evaluate the Oxidative Potential of Atmospheric Aerosols. Atmosphere, 10 (10), 571.

Kelly, F.J., Fuller, G.W., Walton, H.A., Fussell, J.C., 2012. Monitoring air pollution: use of early warning systems for public health. Respirology 17 (1), 7-19.

Kyllönen, K., Vestenius, M., Anttila, P., Makkonen, U., Aurela, M., Wängberg, I., Mastromonaco, M.N., Hakola, H., 2020. Trends and source apportionment of atmospheric heavy metals at a subarctic site during 1996–2018. Atmos. Environ., 236, 117644.

Kim, K.H., Kabir, E., Kabir, S., 2015. A review on the human health impact of airborne particulate matter. Environ. Int. 74, 136143.

Lelieveld, J., Evans, J.S., Fnais, M., Giannadaki, D., Pozzer, A., 2015. The contribution of outdoor air pollution sources to premature mortality on a global scale. Nature, 525, 367.

Lelieveld, J., Klingmüller, K., Pozzer, A., Pöschl, U., Fnais, M., Daiber, A., Münzel, T., 2019. Cardiovascular disease burden from ambient air pollution in Europe reassessed using novel hazard ratio functions. Eur. Heart J. 40, 1590–1596.

Li, R., Kou, X., Geng, H., Xie, J., Yang, Z., Zhang, Y., Cai, Z., Dong, C., 2015. Effect of ambient PM 2.5 on lung mitochondrial damage and fusion/fission gene expression in rats. Chem. Res. Toxicol. 28, 408-418.

Lionetto, M.G., Guascito, M.R., Caricato, R., Giordano, M.E., De Bartolomeo, A.R., Romano, M.P., Conte, M., Dinoi, A., Contini, D., 2019. Correlation of Oxidative Potential with Ecotoxicological and Cytotoxicological Potential of PM10 at an Urban Background Site in Italy. Atmosphere, 10, 733.

Lionetto, M.G., Guascito, M.R., Giordano, M.E., Caricato, R., De Bartolomeo, A.R., Romano, M.P., Conte, M., Dinoi, A., Contini, D., 2021. Oxidative Potential, Cytotoxicity, and Intracellular Oxidative Stress Generating Capacity of PM10: A Case Study in South of Italy. Atmosphere, 12 (4), 464.

Liu, W., Xu, Y., Liu, W., Liu, Q., Yu, S., Liu, Y., Wang, X., Tao, S., 2018. Oxidative potential of ambient PM2.5 in the coastal cities of the Bohai Sea, northern China: Seasonal variation and source apportionment. Environ. Pollut., 236, 514–528.

Manigrasso, M., Soggiu, M.E., Settimo, G., Inglessis, M., Protano, C., Vitali, M., Avino, P., 2022. PM Dimensional Characterization in an Urban Mediterranean Area: Case Studies on the Separation between Fine and Coarse Atmospheric Aerosol. Atmosphere , 13, 227.

Marenco, F., Bonasoni, P., Calzolari, F., Ceriani, M., Chiari, M., Cristofanelli, P., D'Alessandro, A., Fermo, P., Lucarelli, F., Mazzei, F., Nava, S., Piazzalunga, A., Prati, P., Valli, G., Vecchi, R., 2006. Characterization of atmospheric aerosols at Monte Cimone, Italy, during summer 2004: source apportionment and transport mechanism. J. Geophys. Res. 111, D24202.

Massimi, L., Ristorini, M., Simonetti G., Frezzini, M.A., Astolfi, M.L., Silvia Canepari., 2020. Spatial mapping and size distribution of oxidative potential of particulate matter released by spatially disaggregated sources. Environ. Poll., 266, 3,115271.

Matawle, J.L., Pervez, S., Dewangan, S., Shrivastava, A., Tiwari, S., Pant, P., Deb, M.K. and Pervez, Y., 2015. Characterization of PM2.5 Source Profiles for Traffic and Dust Sources in Raipur, India. Aerosol Air Qual. Res., 15, 2537-2548.

Merico, E., Cesari, D., Dinoi, A., Gambaro, A., Barbaro, E., Guascito, M.R., Giannossa, L.C., Mangone, A., Contini, D., 2019. Inter-comparison of carbon content in PM10 and PM2.5 measured with two thermo-optical protocols on samples collected in a Mediterranean site. Environ. Sci. Pollut. Res. 26, 29334–29350.

Mukhtar, A.; Limbeck, A., 2013. Recent developments in assessment of bio-accessible trace metal fractions in airborne particulate matter: A review. Anal. Chim. Acta, 774, 11–25.

Øvrevik, J., 2019. Oxidative Potential Versus Biological Effects: A Review on the Relevance of Cell-Free/Abiotic Assays as Predictors of Toxicity from Airborne Particulate Matter. Int. J. Mol. Sci. 20, 4772.

Paatero, P., Hopke, P.K., 2003. Discarding or down weighting high-noise variables in factor analytic models. Anal. Chim. Acta, 490, 277-289.

Paatero, P., Eberly, S., Brown, S.G., Norris, G.A., 2014. Methods for estimating uncertainty in factor analytic solutions. Atmos. Meas. Tech. 7 (3), 781–797.

Paraskevopoulou, D., Bougiatioti, A., Stavroulas, I., Fang, T., Lianou, M., Liakakou, E., Gerasopoulos, E., Weber, R., Nenes, A., Mihalopoulos, N., 2019. Yearlong variability of oxidative

potential of particulate matter in an urban Mediterranean environment. Atmos. Environ., 206, 183-196.

Perrino, C., Catrambone, M., Dalla Torre S., Rantica, E., Sargolini, T., Canepari, S., 2014. Seasonal variations in the chemical composition of particulate matter: a case study in the Po Valley. Part I: macro-components and mass closure. Environ. Sci. Pollut. Res., 21, 3999-4009.

Perrone, M.R., Bertoli, I., Romano, S., Russo, M., Rispoli, G., Pietrogrande, M.C., 2019. PM2.5 and PM10 oxidative potential at a Central Mediterranean Site: Contrasts between dithiothreitol- and ascorbic acid-measured values in relation with particle size and chemical composition. Atmos. Environ., 210, 143–155.

Pietrogrande, M.C., Perrone, M.R., Manarini, F., Romano, S., Udisti, R., Becagli, S., 2018. PM10 oxidative potential at a Central Mediterranean Site: Association with T chemical composition and meteorological parameters. Atmos. Environ., 188, 97–111.

Pietrogrande, M.C., Bertoli, I., Clauser, G., Dalpiaz, C., Dell'Anna, R., Lazzeri, P., Lenzi, W., Russo, M., 2021. Chemical composition and oxidative potential of atmospheric particles heavily impacted by residential wood burning in the alpine region of northern Italy. Atmos. Environ., 253, 118360.

Pio, C., Cerqueira, M., Harrison, R.M., Nunes, T., Mirante, F., Alves, C., Oliveira, C., Sanchez de la Campa, A., Artinano, B., Matos, M., 2011. OC/EC ratio observations in Europe: re-thinking the approach for apportionment between primary and secondary organic carbon. Atmos. Environ., 45, 6121-6132.

Pope, C.A., Turner, M.C., Burnett, R.T., Jerrett, M., Gapstur, S.M., Diver, W.R., Krewski, D., Brook R.D., 2015. Relationships between fine particulate air pollution, cardiometabolic disorders, and cardiovascular mortality. Circ. Res., 116, 108–115.

Prospero, J.M., Lamb, P.J., 2003. African droughts and dust transport to the Caribbean: Climate change implications. Science 302, 1024–1027.

Querol, X., Alastuey, A., Rodríguez, S., Plana, F., Ruiz, C.R., Cots, N., Massague, G., Puig, O., 2001. PM10 and PM2.5 source apportionment in the Barcelona Metropolitan area, Catalonia, Spain. Atmos. Environ. 35, 6407–6419.

Rodríguez, S., Alastuey, A., Querol, X., 2012. A review of methods for long term in situ characterization of aerosol dust. Aeolian Res., 6, 55-74.

Romano, S., Becagli, S., Lucarelli, F., Russo, M., and Pietrogrande, M.C., 2020. Oxidative Potential Sensitivity to Metals, Br, P, S, and Se in PM10 Samples: New Insights from a Monitoring Campaign in Southeastern Italy. Atmosphere, 11, 367.

Rönkkö, T.J., Hirvonen, M.-R., Happo, M.S., Ihantola, T., Hakkarainen, H., Martikainen, M.-V., Gu, C., Wang, Q.'g., Jokiniemi, J., Komppula, M., Jalava, P.I., 2021. Inflammatory responses of urban air PM modulated by chemical composition and different air quality situations in Nanjing, China. Environ. Res. 192, 110382.

Shiraiwa, M., Ueda, K., Pozzer, A., Lammel, G., Kampf, C.J., Fushimi, A., Enami, S., Arangio, A.M., Fröhlich-Nowoisky, J., Fujitani, Y., Furuyama, A., Lakey, P.S.J., Lelieveld, J., Lucas, K., Morino,

Y., Pöschl, U., Takahama, S., Takami, A., Tong, H., Weber, B., Yoshino, A., Sato, K., 2017. Aerosol health effects from molecular to global scales. Environ. Sci. Technol., 51, 13545–13567.

Simonetti, G., Conte, E., Perrino, C., Canepari, S., 2018. Oxidative potential of size-segregated PM in a urban and an industrial area of Italy. Atmos. Environ., 187, 292-300.

Smirnov, A., Holben, B.N., Savoie, D., Prospero, J.M., Kaufman, Y.J., Tanre, D., Eck, T.E., Slutsker, I., 2000. Relationship between column aerosol optical thickness and in-situ ground based dust concentrations over Barbados. Geophys. Res. Lett., 27, 1643–1646.

USEPA. The National Ambient Air Quality Standards (NAAQS) for Particulate Matter (PM): EPA's 2006 Revisions and Associated Issues; Congressional Research Service. 2013. Available online: https://sgp.fas.org/crs/misc/RL34762.pdf (accessed on 26 October 2021).

Valavanidis, A., Fiotakis, K., Vlachogianni, T., 2008. Airborne particulate matter and human health: toxicological assessment and importance of size and composition of particles for oxidative damage and carcinogenic mechanisms. J. Environ. Sci. Health C Environ. Carcinog. Ecotoxicol. Rev., 26 (4), 339–362.

Verma, V., Fang, T., Xu, L., Peltier, R.E., Russell, A.G., Ng, N.L., Weber, R.J., 2015. Organic Aerosols Associated with the Generation of Reactive Oxygen Species (ROS) by Water-Soluble PM2.5. Environ. Sci. Technol., 49, 4646−4656

Visentin, M., Pagnoni, A., Sarti, E., Pietrogrande, M.C., 2016. Urban PM2.5 oxidative potential: Importance of chemical species and comparison of two spectrophotometric cell-free assays. Environ. Poll., 219, 72-79.

Waked, A., Bourin, A., Michoud, V., Perdrix, E., Alleman, L.Y., Sauvage, S., Delaunay, T., Vermeesch, S., Petit, J.E., Riffault, V., 2018. Investigation of the geographical origins of PM10 based on long, medium and short-range air mass back-trajectories impacting Northern France during the period 2009–2013. Atmos. Environ.,193, 143-152.

Weber, S., Uzu, G., Calas, A., Chevrier, F., Besombes, J.L., Charron, A., Salameh, D., Ježek, I., Močnik, G., Jaffrezo, J.L., 2018. An apportionment method for the oxidative potential of atmospheric particulate matter sources: Application to a one-year study in Chamonix, France. Atmos. Chem. Phys., 18, 9617–9629.

Weber, S., Uzu, G., Favez, O., Borlaza, L.J.S., Calas, A., Salameh, D., Chevrier, F., Allard, J., Besombes, J.L., Albinet, A., Pontet, S., Mesbah, B., Gille, G., Zhang, S., Pallares, C., Leoz-Garziandia, E., Jaffrezo, J.L., 2021. Source apportionment of atmospheric PM10 oxidative potential: synthesis of 15 year-round urban datasets in France. Atmos. Chem. Phys., 21, 11353–11378.

WHO, 2013. Review of Evidence on Health Aspects of Air Pollution e REVIHAAP. First Results. WHO's Regional Office for Europe, Copenhagen, p. 28, 2013. http://www.euro.who.int/data/assets/pdf_file/0020/182432/e96762-final.pdf.

WHO, 2021, WHO global air quality guidelines. Particulate matter (PM2.5 and PM10), ozone, nitrogen dioxide, sulfur dioxide and carbon monoxide. Geneva: World Health Organization; 2021. Licence: CC BY-NC-SA 3.0 IGO.

Yang, Y., Lou, S., Wang, H., Wang, P., Liao, H., 2020. Trends and source apportionment of aerosols in Europe during 1980–2018. Atmos. Chem. Phys. 20, 2579–2590.

Yang, F, Liu, C, Qian, H, 2021. Comparison of indoor and outdoor oxidative potential of PM2.5: pollution levels, temporal patterns, and key constituents. Environ. Int., 155, 106684.

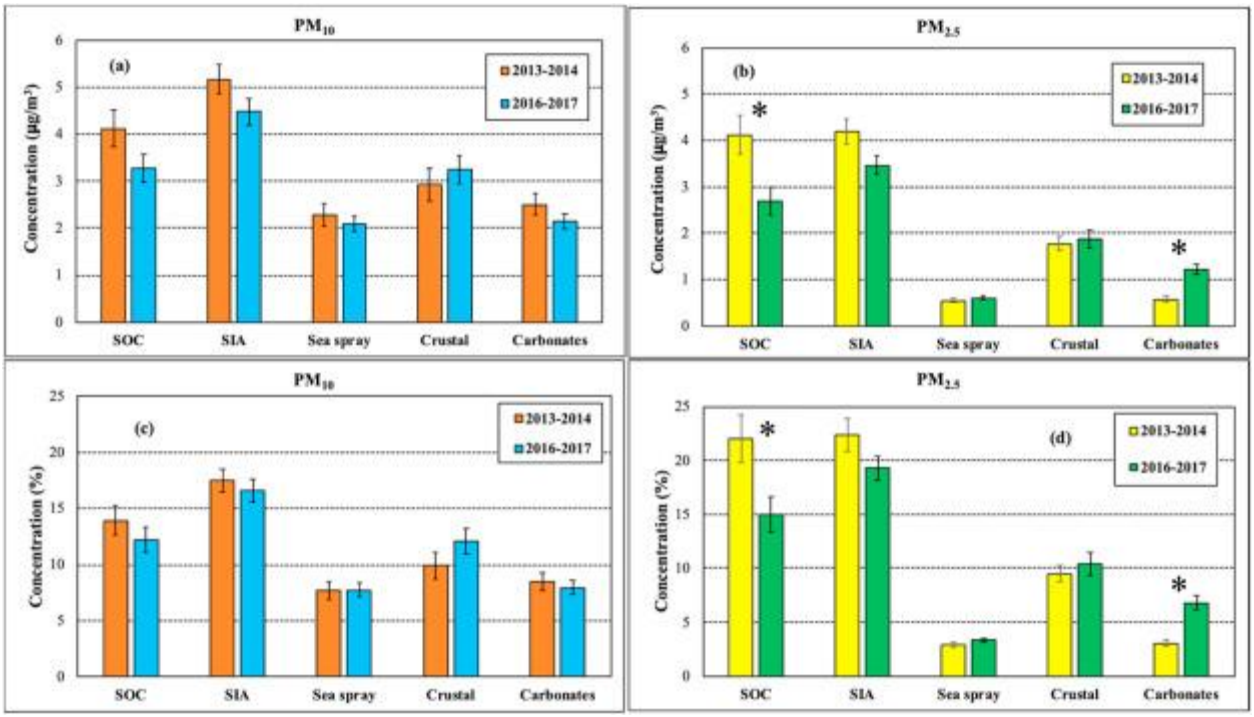

Fig. 1. Variability of absolute (μg/m^3) and relative (%) concentrations of secondary species, SOC and SIA, sea spray, crustal and carbonates contributions in PM_{10} (a, c) and in $PM_{2.5}$ (b, d). Errors bars represent the variabilities in terms of standard errors. * p-value < 0.05 (ANOVA test).

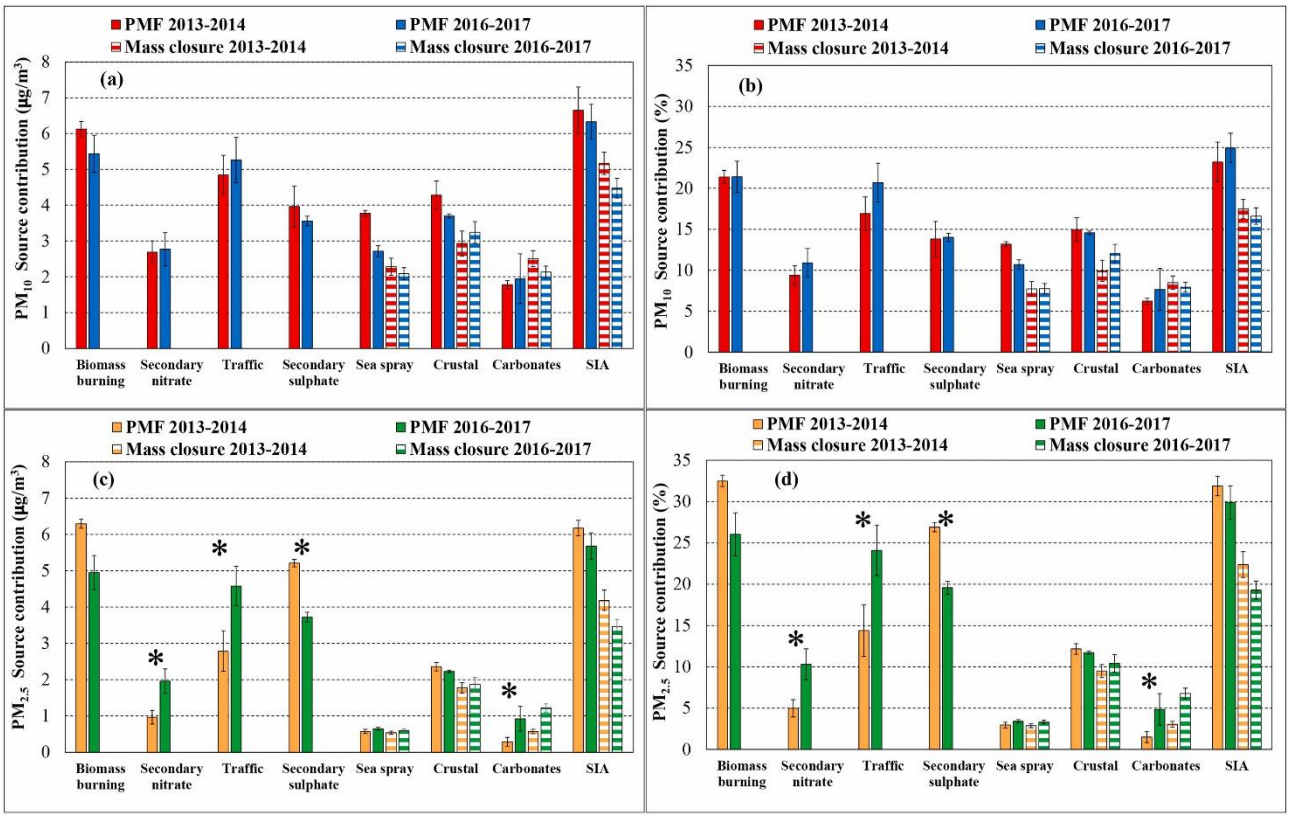

Fig. 2. Comparison of PM source contributions, in absolute (a, c), and relative terms (b, d), obtained with the two dataset 2013–2014 and 2016–2017. * p-value < 0.05 (ANOVA test).

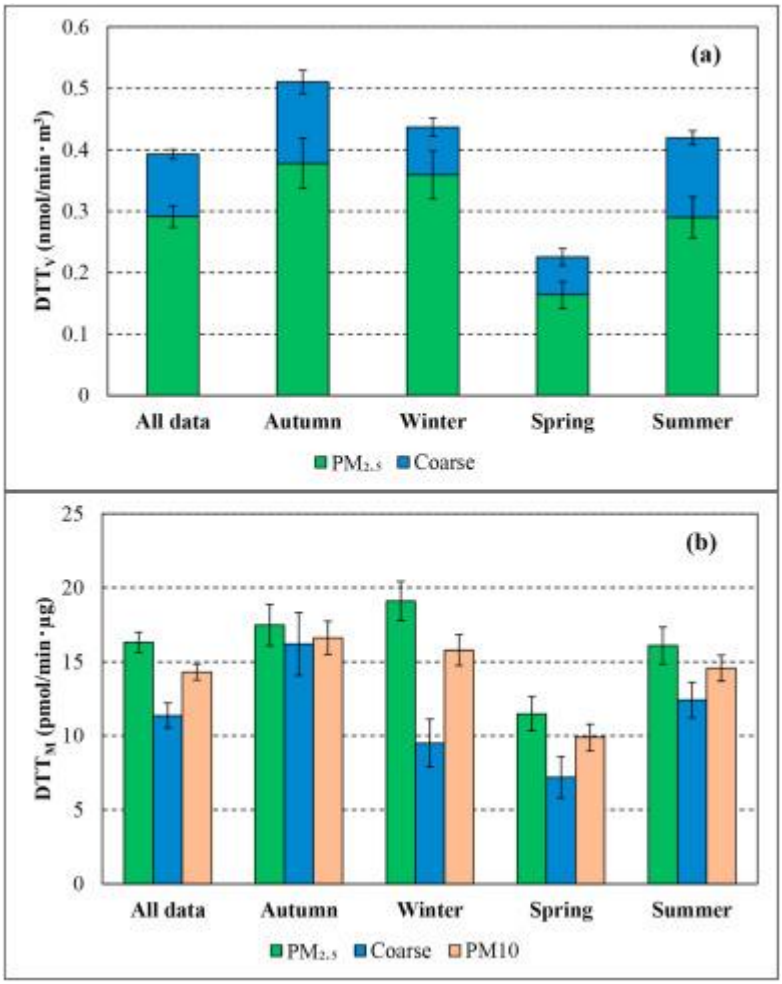

Fig. 3. (a) Seasonal variability of DTT_V (nmol/min·m^3) for $PM_{2.5}$ and for the coarse ($PM_{10-2.5}$) fraction. (b) DTT_M activity (pmol/min·µg) for $PM_{2.5}$, PM_{10}, and coarse fraction for the entire 2016–2017 period. Errors bars represent the variabilities in terms of standard errors.

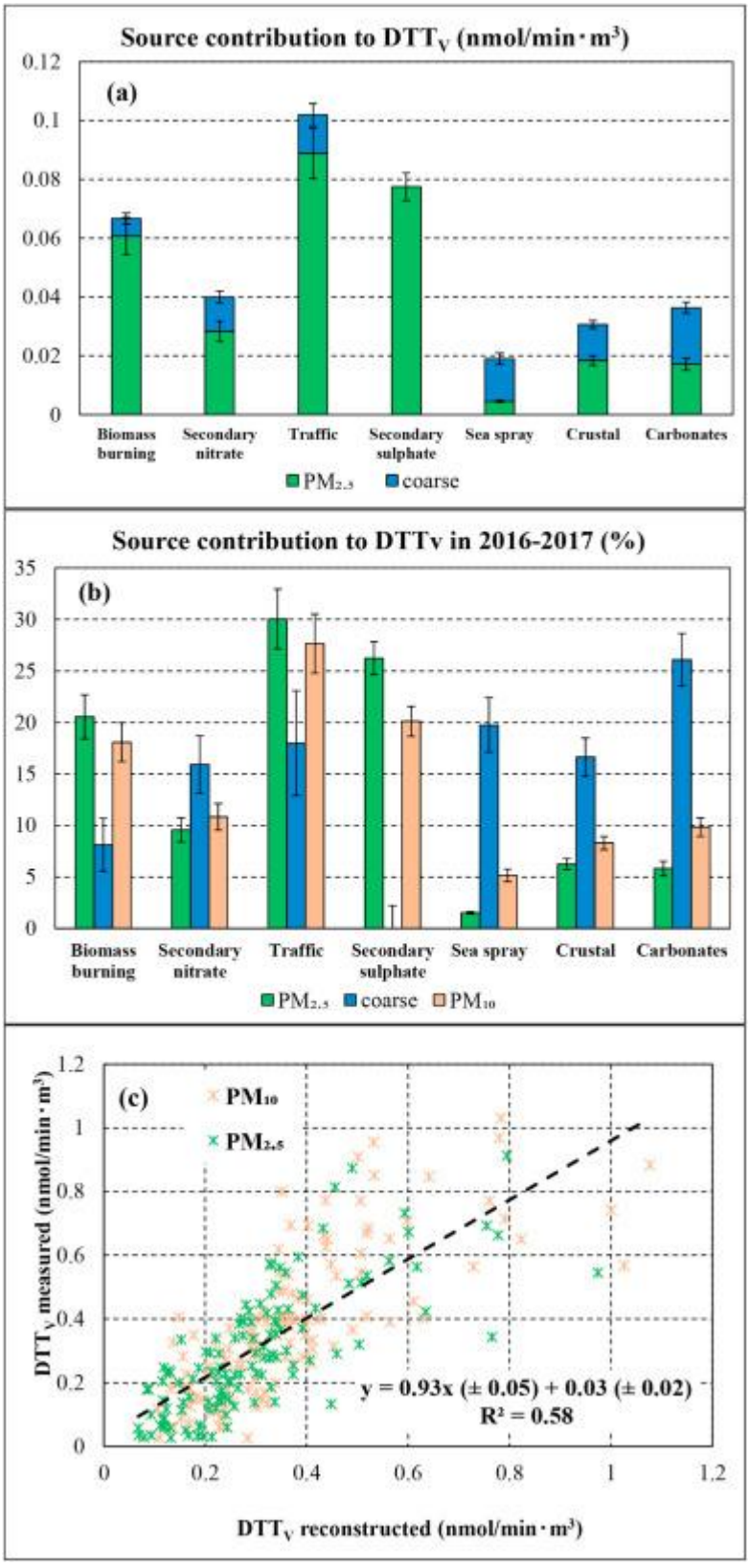

Fig. 4. (a) Absolute source contributions to DTT_V in $PM_{2.5}$ and coarse fraction obtained using the MLR approach. (b) Source contributions in relative terms for $PM_{2.5}$, PM_{10}, and coarse fraction. (c) Comparison between measured and reconstructed DTT_V including a linear fit. Errors bars represent the variabilities in terms of standard errors.